

Strengthening of bolted shear joints in industrialized ferrocement construction

M. Ismail^{1b}, M. Shariati^{*1,2,3}, A.S.M. Abdul Awal^{1a}, C.E. Chiong^{4a},
E. Sadeghipour Chahnasir⁵, A. Porbar⁵, A. Heydari^{6b} and M. Khorami^{7b}

¹ Faculty of Civil Engineering, Universiti Teknologi Malaysia, Johor Bahru, Malaysia

² Faculty of Civil Engineering, University of Tabriz, Tabriz, Iran

³ Department of Civil Engineering, University of Malaya, 50603, Kuala Lumpur, Malaysia

⁴ Faculty of Civil and Environmental Engineering, Universiti Tun Hussein Onn, Malaysia

⁵ Department of Civil Engineering, Qeshm International Branch, Islamic Azad University, Qeshm, Iran

⁶ Young Researchers and Elite Club, Ardabil Branch, Islamic Azad University, Ardabil, Iran

⁷ Facultad de Arquitectura y Urbanismo, Universidad Tecnológica Equinoccial, Calle Rumipamba s/n y Bourgeois, Quito170508, Ecuador

(Received April 15, 2017, Revised April 25, 2018, Accepted July 6, 2018)

Abstract. This paper highlights results of some experimental work that deals with strengthening of bolted shear joints in thin-walled ferrocement structure where steel wires, bent into U-shape are considered as simple inserts around the bolt hole. The parameters investigated include the number of layers of wire mesh, edge distance of bolt hole, size and location of the inserts. Test results have shown that for small edge distance, failure occurred either in cleavage or shearing mode, and the strength of the joint increased with an increase in the edge distance. This continued up to an upper limit set by either tension or bearing failure. The experimental study further revealed that for a given edge distance the strength of a joint can significantly be enhanced by using U-inserts. The equations developed for predicting joint strength in ferrocement composites can also be modified to include the effects of the inserts with a good level of accuracy.

Keywords: ferrocement; composite structure; bolt; shear joint; strength

1. Introduction

Many researches are conducted for improving structural behaviors by applying new ideas. For example, the effects of ductility on behavior of braced frames (Andalib *et al.* 2010, 2011, Bazzaz 2010, Bazzaz *et al.* 2011a, b, 2012a, 2012b, 2014, 2015, Fanaie *et al.* 2012, 2016a, b, Mohammadhassani *et al.* 2015, Mansouri *et al.* 2016, Momenzadeh *et al.* 2017) or composite beams (Shariati 2013, Shariati *et al.* 2013, 2014a, b, 2018, Fanaie *et al.* 2015, Khorramian *et al.* 2015, 2017, Shariati *et al.* 2015, 2016, Shahabi *et al.* 2016, Tahmasbi *et al.* 2016, Jamkhaneh and Kafi 2017, Hosseinpour *et al.* 2018, Ma *et al.* 2018) are studied extensively.

Novel and various approaches have been used for this purpose (Mohammadhassani *et al.* 2013, 2014, Toghroli *et al.* 2014, 2016, Safa *et al.* 2016, Khorami *et al.* 2017a, b, Stanojevic *et al.* 2017). There are various benefits over the conventional structural materials and analysis methods (Heydari and Shariati 2018, Toghroli *et al.* 2018). In recent years, ferrocement composite has made remarkable advances not only in the utilization of advanced materials and composites, but also in various aspects of its manufacture. Mechanized fabrication of reinforcement

cages, employment of modern precast technology and use of bolted connections to assemble precast units have transformed ferrocement, once regarded as a low-tech construction material, into a quality material of choice in many practical applications (Abdul Awal 1988, Balaguru and Batson 1997, Naaman 2000, Shah 2011, Mourad and Shannag 2012, Li *et al.* 2013). Among the advanced technologies applied to ferrocement, the concept of connecting the thin-walled concrete elements by bolts has opened up new possibilities for exploring innovative applications embracing high-level industrialized construction techniques. One such application conceptually arrived at is the construction of a two-storey housing system using precast channels and half-box panels (Naaman 1989, Naaman and Hammoud 1992). It has been proposed that these prefabricated elements can be assembled on site by using bolts instead of a wet joint (Mansur *et al.* 1987, Krishnamoorthy *et al.* 1990, Murali 1997, Li *et al.* 2018). One of the most common types of joints in such a structural system is 'shear type' joint.

Tests conducted in the past (Abdullah and Alwis 1994, Mansur 1995, Katula and Dunai 2015, Ksentini *et al.* 2015, Lopez-Arancibia *et al.* 2015, Guo *et al.* 2016a, b) have revealed that this type of joints may fail in four different modes: tension, cleavage, shear and bearing, as shown in Fig. 1. Based on plasticity theory, analytical expressions for estimating the strength of a joint failing in tension or shear were also proposed by Abdullah and Alwis (1994), while Hammoud and Naaman (1998, 2000) proposed a simple expression based on finite element analysis to predict the

*Corresponding author, Ph.D.,
E-mail: mahdishariati@utm.my

^a Ph.D.

^b Ph.D. Student

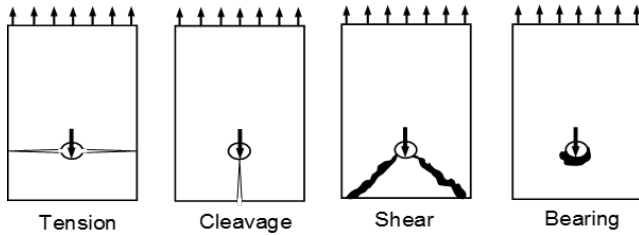


Fig. 1 Various modes of joint failure

strength of a joint failing in cleavage mode. With the establishment of the bolt-bearing strength of ferrocement through a comprehensive investigation by Mansur *et al.* (2001), the technical information necessary to accomplish rational design of a bolted shear joint is now available. The expressions predicting the ultimate strength P_t , P_{cb} , P_s , and P_b of a joint failing respectively in tension, cleavage, shear and bearing may be summarized as follows

Tension mode of failure:

$$P_t = h(w - d)f_t \tag{1}$$

Cleavage mode of failure:

$$P_{cl} = 1.67h(e - 0.5d)f_t \tag{2}$$

Shear mode of failure:

$$P_s = eh(f_t f_c^*)^{0.5} \tag{3}$$

Bearing mode of failure:

$$P_b = 2f_c'hd \tag{4}$$

in which, e is the edge distance of the bolt hole, h is the thickness of joint specimens, w is the width of plate, d is the diameter of bolt hole, f_t is the tensile strength of ferrocement composite, f_c' is the compressive strength of the composite, which may be taken same as the cylinder compressive strength of mortar, and f_c^* is the reduced compression capacity of the mortar due to the existence of perpendicular tension $= \nu f_c$. The recommended value of the reduction factor, ν for ferrocement is 0.53 (Naaman and Hammoud 1992). A close scrutiny of these equations reveals that the strength of a given joint with known geometry and strength properties of the composite that fails in either tension or cleavage modes is governed by tensile strength, f_t of the composite, while that failing in bearing is governed by its compressive strength, f_c' . In contrast, the shearing mode of failure is governed by both tensile and compressive strength of the composite. In cement-based composites, the tensile strength is solely provided by the reinforcement.

Therefore, the strength of a joint failing in any of the three modes - tension, cleavage or shear can be enhanced by using simple inserts around the bolt hole. When suitably placed, the insert will contribute to f_t , thus improving the capacity and efficiency of the joint without having to change its geometry or details of the members being connected. A previous attempt to strengthen a shear joint by

embedding steel pipes to pre-form the bolt hole was not successful (Mansur 1995). The present investigation on bolted shear joint in ferrocement has been directed towards exploring the extent of strengthening that can be accomplished by incorporating simple U-shaped steel inserts around the bolt-hole.

2. Experimentation

2.1 Test program

In all, 28 ferrocement plate specimens in the form of symmetric butt joints were tested in direct tension. Each specimen was 400 mm long, 150 mm wide and 20 mm thick. They were symmetrically reinforced across the thickness and contained 2 bolt holes near two ends, one being 16 mm in diameter (test hole) and the other 20 mm (Fig. 2). The region near the 20 mm bolt hole was strengthened with additional wire mesh to ensure that the failure would take place at or around the 16 mm diameter test bolt hole. The general view of the test setup is illustrated in Fig. 3.

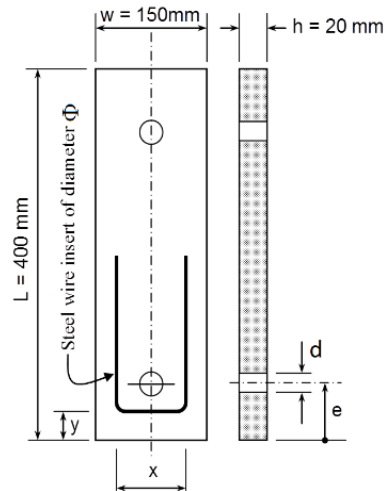


Fig. 2 Specimen details with U-insert

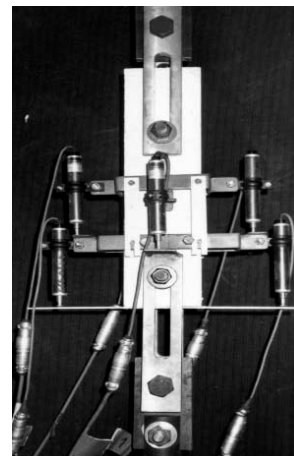


Fig. 3 A view of test setup.

Table 1 Test program and specimen details

S1. No.	Series	Group	Specimen	Number of mesh\ layers, N	*Details of steel insert			* <i>e</i> (mm)					
					Diameter, Φ (mm)	Dimension, <i>x</i> (mm)	Distance, <i>y</i> (mm)						
1	U (Un-strengthened)	UA	N4-E35	4	0	N/A	N/A	35					
2			N4-E50					50					
3			N4-E65					65					
4			N4-E80					80					
5			N4-E95					95					
6			N4-E110					110					
7		UB	N2-E35	2	4	25	5	35					
8			N2-E50					50					
9			N2-E65					65					
10			N2-E80					80					
11			N2-E95					95					
12			N2-E110					110					
13	S (Strengthened with U-inserts)	SB	D4-X25-Y5-E35	2	4	25	5	35					
14			D4-X25-Y5-E50					50					
15			D4-X25-Y5-E65					65					
16			D4-X25-Y5-E80					80					
17			D4-X25-Y5-E95					95					
18			D4-X25-Y5-E110					110					
19		SD	D3-X25-Y5-E35	2	4	25	5	35					
20			D3-X25-Y5-E50					50					
21			D5-X25-Y5-E35					35					
22			D5-X25-Y5-E50					50					
23			SY					D4-X25-Y15-E35	2	4	25	5	35
24								D4-X25-Y15-E50					50
25	SX	D4-X50-Y5-E35	2	4	25	5	35						
26		D4-X50-Y5-E50					50						
27		D4-X75-Y5-E35					35						
28		D4-X75-Y5-E50					50						

*Refer to Fig. 2

Table 1 shows details of the test program. In the test program the specimens are divided into two series, S and U, designating specimens with and without strengthening by using steel wire insert. Each series is subsequently divided into a number of groups investigating a particular test parameter. The major parameters considered include the number of layers of wire mesh, *N*, edge distance, *e*, of the bolt hole, wire diameter, Φ , of U-shaped insert similar to a staple, the dimension of insert between the two outstanding legs, *x*, and the distance *y* of the insert from the free edge defining its placement in the joint (Refer to Fig. 2). Each specimen is designated by the above test parameters in capital letters, each followed by a numeral indicating its value in millimeters, where applicable.

Specimens in the basic series U were divided into two groups, UA and UB, depending on the number of layers of

wire mesh, 4 and 2, respectively. Each of these groups contained six identical specimens in which the edge distance, *e*, of the bolt hole was varied from 35 mm to 110 mm at an increment of 15 mm, as can be seen in Table 1. Strengthened specimens in Group SB are identical to those of the corresponding specimen in Group UB, except that each of these specimens contained a steel wire insert of 4 mm diameter having the dimension, *x* = 25 mm and placed at *y* = 5 mm.

The strengthened specimens in the remaining Groups SD, SY, and SX were identical to those in Group SB with only two positions of the bolt hole, that is, *e* equal to 35 and 50 mm. The differences were in the diameter of insert wire Φ , placement distance *y*, from the edge of the plate, and the dimension *x* of the insert for the specimens in Groups SD, SY and SX, respectively.

2.2 Materials and preparation of specimens

Galvanized welded wire mesh of 12.5-mm square openings and 1.42-mm wire diameter was used as reinforcement throughout the test program. Three different

sizes of steel wires of 3 mm, 4 mm, and 5 mm in diameter, bent in U-shape (staple) were used as steel insert around the bolt hole (Fig. 2). Tension tests were conducted on representative mesh samples and individual steel wires. The average yield strength, based on 0.2% permanent strain, and the ultimate strength obtained are presented in Table 2.

All specimens were symmetrically reinforced across the thickness with a clear mortar cover of 3 mm, and the steel inserts were placed in the middle. Bolt holes were performed by inserting same diameter bolt through the circular opening drilled through the plywood molds at appropriate locations. One longitudinal and one transverse wire from each layer of mesh had to be cut to make room for the bolt hole. Ordinary Portland cement, natural sand passing through ASTM sieve No. 16 (1.18 mm) and fineness

Table 2 Strength of various types of steel

Type of steel	Yield strength, f_y (MPa)	Ultimate strength, f_u (MPa)
Wire Mesh	361	447
3 mm diameter wire	566	668
4 mm diameter wire	502	590
5 mm diameter wire	510	541

Table 3 Test data and comparison with theoretical predictions

No.	Specimen	Mortar strength f_c (MPa)	Mode of failure	Experimental		Calculated		$\frac{P_u, \text{expt}}{P_u, \text{calc}}$
				Load		Mode of failure	P_u, calc (kN)	
				First cracking (kN)	P_u, expt (kN)			
1	N4-E35	37.7	S/C	5.9	9.15	C	8.25	1.11
2	N4-E50	37.7	S/C	6	14.03	C	12.83	1.09
3	N4-E65	37.7	S/C	6.7	19.48	C	17.41	1.12
4	N4-E80	37.7	S	7	23.31	S	21.63	1.08
5	N4-E95	37.7	T/B	8.6	28.22	T	24.13	1.17
6	N4-E110	37.7	T/B	9.3	29.31	T	24.13	1.21
7	N2-E35	37.9	S/C	5.4	6.56	C	4.12	1.59
8	N2-E50	37.9	S/C	5.62	9.32	C	6.42	1.45
9	N2-E65	37.9	C	6.5	11.87	C	8.71	1.36
10	N2-E80	37.9	T/C	8.41	14.4	C	11	1.31
11	N2-E95	37.9	T	8.5	15.11	T	12.26	1.23
12	N2-E110	37.9	T	9.01	15.51	T	12.26	1.27
13	D4-X25-Y5-E35	37.1	S	6	10.3	S	9.46	1.09
14	D4-X25-Y5-E50	37.1	S	7.31	14.11	C	13.51	1.04
15	D4-X25-Y5-E65	37.1	S	5.8	17.45	C	17.56	0.99
16	D4-X25-Y5-E80	37.1	S	8.8	21.01	C	21.53	0.98
17	D4-X25-Y5-E95	37.1	T	9.2	23.81	C	23.74	1
18	D4-X25-Y5-E110	37.1	T	9.5	22.58	C	23.74	0.95
19	D3-X25-Y5-E35	41	S/C	5.81	8.5	C	8.97	0.95
20	D3-X25-Y5-E50	41	S	7.52	13.2	C	12.82	1.03
21	D5-X25-Y5-E35	41	S/C	6.61	14.8	S	11.33	1.31
22	D5-X25-Y5-E50	41	S	8.51	18.9	C	16.18	1.17
23	D4-X25-Y15-E35	41	S	6.11	13.21	S	9.94	1.33
24	D4-X25-Y15-E50	41	S	6.18	14.34	C	14.2	1.01
25	D4-X50-Y5-E35	39.4	S	5.59	11.82	S	9.75	1.21
26	D4-X50-Y5-E50	39.4	S	8.45	16.5	C	13.92	1.19
27	D4-X75-Y5-E35	39.4	S	5.32	13.01	S	9.75	1.34
28	D4-X75-Y5-E50	39.4	S/C	7.09	16.7	C	13.92	1.2
							Average	1.17
							Standard deviation	0.16

modulus of 3.15 was used. The sand-cement ratio by weight was 2:1 and water-cement ratio was 0.55 throughout the study.

The specimens were cast on a vibrating table by placing the mold vertically on one of its sides. Six 100×200 mm control cylinders were cast for each batch of mortar to determine its compressive strength. The hole-forming bolts were removed 3 hours after casting. Upon stripping off the molds 24 hours later, the specimens together with the control cylinders were moist cured for six days followed by air-curing in the laboratory before testing. The average cylinder compressive strengths at the time of testing of parent specimens are presented in Table 3.

2.3 Instrumentation and test procedure

The tests were conducted in a 50-ton capacity servo controlled Instron testing machine. The bolted specimen was loaded via steel links, as shown in Fig. 3. The bolt material and size of the bolts were selected to preclude bolt distress prior to failure of the ferrocement plate material. A set of four LVDT's is used to acquire information on specimen deformation, particularly the displacement of the bolt. A preload of 100 N was applied to the specimen before the bolts were tightened in order to avoid initial load eccentricity. In all cases, the nut was tightened to finger tight condition with washers on both sides of the specimens. The internal diameter of the washer was 17.8 mm, while the external diameter was 38.6 mm, the thickness being 3.45 mm. The load was applied with a constant cross head displacement rate of 0.1 mm/min. The initiation crack was carefully observed and the corresponding load was recorded. The ultimate load and mode of failure were noted after failure.

3. Test result and discussion

3.1 General behavior

Typical load versus bolt displacement curves of the specimens are presented in Fig. 4. It may be seen that the curves are linear up to about the cracking load. In general, cracks were initiated at the hole-boundary due to stress concentration. The loads at which cracks became visible (the bolt hole was partly obstructed by the loading device) ranged from about 40% to 60% of the ultimate load, and these values are shown in Table 3. Cracking was accompanied by a slight decrease in the slope of the curve, but the relationship remained essentially straight. As the load was increased, additional cracks formed and the existing cracks propagated in a radial direction. However, the width of cracks remained quite narrow indicating that the integrity of the joint remained relatively unaffected up to about 80%-90% of the ultimate load. Beyond this load level, cracks started to grow rapidly with increasing load, and the corresponding load-displacement curve started to deviate significantly from linearity, gradually becoming horizontal. Thereafter, bolt displacement increased with associated drop in the applied load. Fig. 5 reveals the cracking patterns of the specimens after failure.

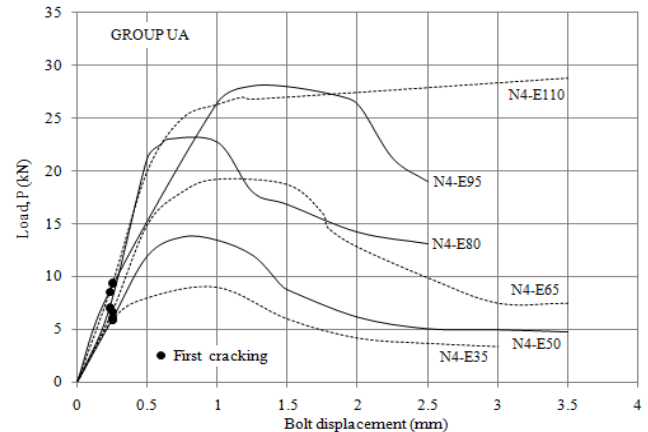


Fig. 4 Typical load vs. bolt displacement curves

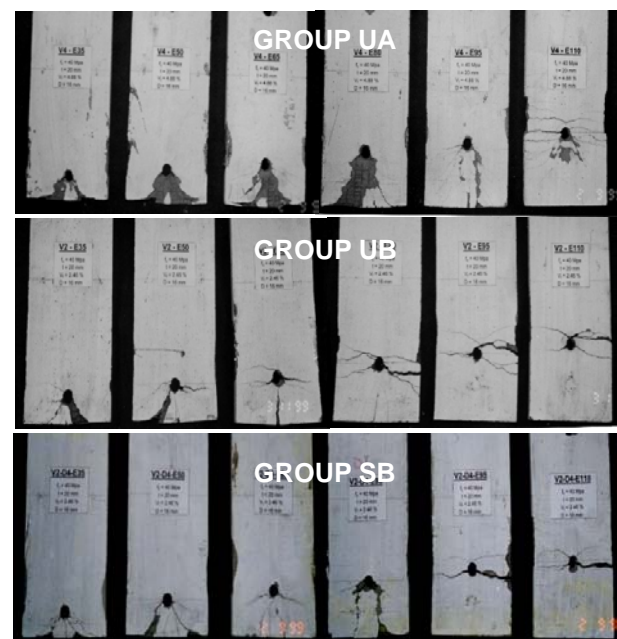


Fig. 5 Typical mode of failure of test specimens

After failure, the specimens were carefully examined for the type and direction of cracking, and crushing of the concrete to identify the mode of failure. Four basic failure modes - tension, cleavage, shear and bearing, as illustrated in Fig. 1 and reported earlier by Mansur et al. (Abdullah and Alwis 1994), have been identified. The modes of failure identified for each specimen are listed in Table 3. It may be seen that the shear failure was the most commonly observed failure mode and in most cases, cleavage failure was associated with shear failure.

3.2 Effect of edge distance, e

It may be recalled that each of the Groups UA, UB and SB consists of six identical specimens, differing only in the edge distance, e , which was varied from 35 mm to 110 mm at an increment of 15 mm (Table 1).

Specimens in Group UA contained four layers of wire mesh, while those in Group UB contained only two layers.

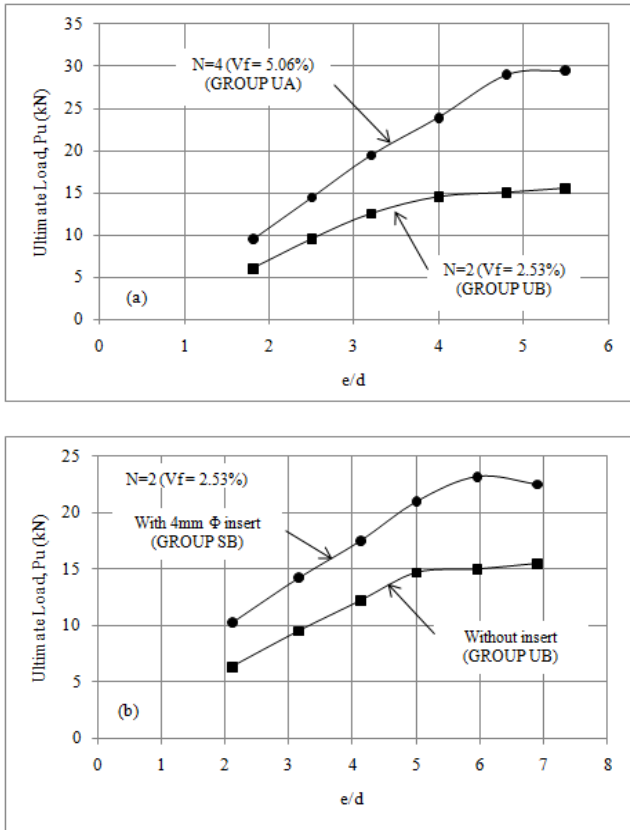


Fig. 6 Effect of (a) volume fraction of reinforcement; and (b) using U-insert on ultimate strength of the joint

The specimens in Group SB were identical to those in Group UB, except that each of these specimens was provided with a 4-mm diameter U-shaped steel-wire insert in an attempt to enhance the joint strength. For the remaining groups, two different e -values, 35 mm and 50 mm were used for two identical specimens.

Referring to Table 3 and Fig. 6, it may be clearly seen that an increase in the value of e increases the joint capacity provided the reinforcement details in and around the bolt hole remains identical. However, this continues only up to a certain value depending on the relative values of tensile and compressive strengths of the composite. Thereafter, joint capacity remains almost constant. As mentioned earlier, shear failure is the most common type of failure when the edge distance is small say, in the present case, less than about 80 mm, and this type of failure is frequently associated with a cleavage mode. Similar observations were reported earlier by Mansur *et al.* (Abdullah and Alwis 1994). For large edge distance, failure occurs either in tension or bearing. Being independent of the value of e (shown in Eqs.1-4), the strength of the joint failing in one of these modes represents the upper bound of the strength of a joint.

3.3 Effect of number of mesh layers, N

The effects of the number of layers of wire mesh or, in other words, the volume fraction of reinforcement may be observed from the results of Groups UA and UB plotted in Fig. 6(a). The specimens in these groups contained 4 and 2

layers of square wire mesh, which corresponded to a total volume fraction of reinforcement of 5.06% and 2.53%, respectively. It may be seen that for a given edge distance, use of a higher volume fraction of reinforcement leads to a higher joint strength for obvious reasons.

A close examination of the failure modes for two groups of specimens presented in Fig. 5 shows that for the small values of e , the shear and cleavage failures are more dominated for Group UA specimens than those are in Group UB, respectively. This indicates that the specimens with low tensile strength (less steel) are more susceptible to cleavage failure. Similarly, these specimens are likely to fail in tension for large values of e . Obviously, the strength of a joint in direct tension increases as the amount of reinforcement is increased, eventually exceeding the bearing strength. This is evidenced by bearing failure of the two specimens with large values of e in Group UA (Fig. 5).

3.4 Effect of U-inserts

Each of the specimens in Group UB contained two layers of wire mesh. The specimens in Group SB were identical to those in UB except that a 4mm-diameter U-shaped steel wire was placed in between the two layers of wire mesh enclosing the bolt hole. This shape was selected to furnish additional reinforcement directly through the critical section for cleavage and tension failure, and to intercept the tapered failure surface in shear. By referring to Fig. 6(b), it may further be noted that the addition of a U-insert for the specimens in Group UB enhanced the strength of the joint up to about 60%. It may be noted that these specimens contained only two layers of wire mesh which corresponds to 2.53% volume fraction of reinforcement. For higher volume fraction of reinforcement, such dramatic improvement in joint strength may not be possible to accomplish because of the possibility of reaching compression capacity of the mortar.

Inclusion of U-inserts also changed the mode of failure, as can be seen in Table 3. In Group UB, signs of cleavage failure (initiation of crack directly below the loading point in a direction parallel to loading) were observed in several instances but, no such sign was displayed by specimens in Group E. The modes of failure for specimens in Group UB were mostly shear and tension. Hence, the addition of U-inserts not only increases the strength of a joint but also reduces the possibility of cleavage type failure.

3.5 Effect of diameter of inserts

Three different sizes of wire-inserts, 3 mm, 4 mm and 5 mm in diameter, were used in this experiment for two values of e , 35 mm and 50 mm (Group SD and specimens 13 and 14, See Table 1). It may be seen in Fig. 7(a) that for a given value of e , an increase in wire size increases the ultimate strength of a joint. However, no change in the modes of failure was noted for the three different sizes of wires used; all six specimens involved demonstrated clear shear failure.

3.6 Effect of dimension and location of inserts

Specimens in Group SX, together with specimens 13

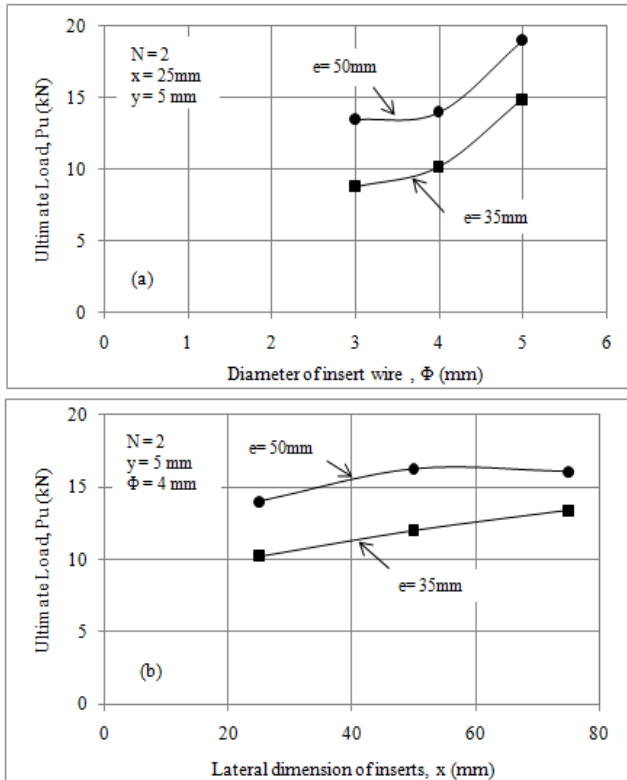


Fig. 7 Effect of (a) diameter, d and (b) lateral dimension, X of U-insert on ultimate strength of the joint

and 14 were used to investigate the effect of changing the dimension x of the inserts. The wire diameter was 4 mm and the distance, x , between the two outstanding legs were 25 mm, 50 mm and 75 mm (half the width of specimen). Specimens 13 and 14 with $y = 5$ mm may also be used with those in Group SY where the insert was placed at $y = 15$ mm to have an idea of the effect of the location of insert on joint strength. Referring to Fig. 7(b) and Table 3, it may be observed that the ultimate strength of joint increases with the increase in the lateral dimension x . An increase in the distance y also occurred for an increase in ultimate strength, but for small value of e (See Table 3). However, for $e = 50$ mm, it is insignificant. Further study, giving a more detailed coverage, is therefore needed to obtain conclusively the effect of y on the joint strength.

4. Comparison of test results with theoretical predictions

The ultimate strength of a bolted shear joint in ferrocement may be analytically calculated by using the equations available in the literature. These equations, summarized here as Eqs. (1)-(4) for the four possible failure modes, may be used with no difficulty for the un-strengthened series, that is, specimens in Groups UA and UB.

In these groups, only the wire mesh contributes to the required tensile strength, f_t of the composite. For square wire mesh, the strength of the composite in direct tension is

the same in any direction, and can be calculated from the following equation

$$f_t = N \frac{A_{sm} f_{ym}}{sh} \quad (5)$$

In which N is the number of layers of wire mesh, s is the grid size of square mesh, A_{sm} is the area of wires in the mesh and f_{ym} is its yield strength. In this case, wire meshes used had square openings. Therefore, the same value of f_t may be taken in any direction.

In case of specimens strengthened with U-inserts (Series S), Eqs. (1) to (4) cannot be directly applied to calculate the capacity of a joint. However, the insert intercepted by the failure surface will contribute to the tensile strength of the composite. If it is assumed that the insert have yielded at failure, then referring to Fig. 1, the contribution of insert may be taken equivalent to two times the yield force of the insert wire for tension failure of the specimens, because two legs are intercepted by the failure crack. Thus, for failure in the tension mode, the tensile strength, f_t , of the composite for specimens strengthened by U-insert is given by

$$f_t = N \frac{A_{sm} f_{ym}}{sh} + \frac{2A_{si} f_{yi}}{wh} \quad (6)$$

In which, A_{si} is the cross sectional area of wire insert, f_{yi} is its yield strength.

Similarly, since the failure crack for the cleavage mode intercept the U-insert only once, the tensile strength of the composite may be obtained by adding the contribution of one leg to that provided by the wire mesh. That is, tensile strength to be used in Eq. (2) may be taken as follows

$$f_t = N \frac{A_{sm} f_{ym}}{sh} + \frac{A_{si} f_{yi}}{(e - d/2)h} \quad (7)$$

The above argument may not hold for shearing mode of failure. Since the outstanding legs of U-inserts are intercepted by the inclined failure line, the tensile strength of the composite as calculated for tension mode of failure (Eq. (6)) to include the effect of insert is assumed for shear failure as well.

For each specimen, the ultimate strengths corresponding to the four possible modes of failure have been calculated using Eqs. (1)-(4) with some modifications for U-inserts represented by Eqs. (5)-(7). The smallest ultimate strength was therefore taken as the failure load and the corresponding mode as the predicted mode of failure.

According to the theory, the mode of failure is governed by either cleavage or shear when the edge distance is small. The predicted load increases linearly until tension (or bearing) mode of failure takes over. Thereafter, the failure load remains constant with increasing edge distance. It can be seen in Table 3 that except for a few cases, the predicted mode of failure is in close agreement with those observed experimentally. Also, the trends of experimental results were similar to the predicted results as shown in Fig. 8. It is interesting to note from Fig. 8, that the difference between experiment and theory is quite large for specimens in Group

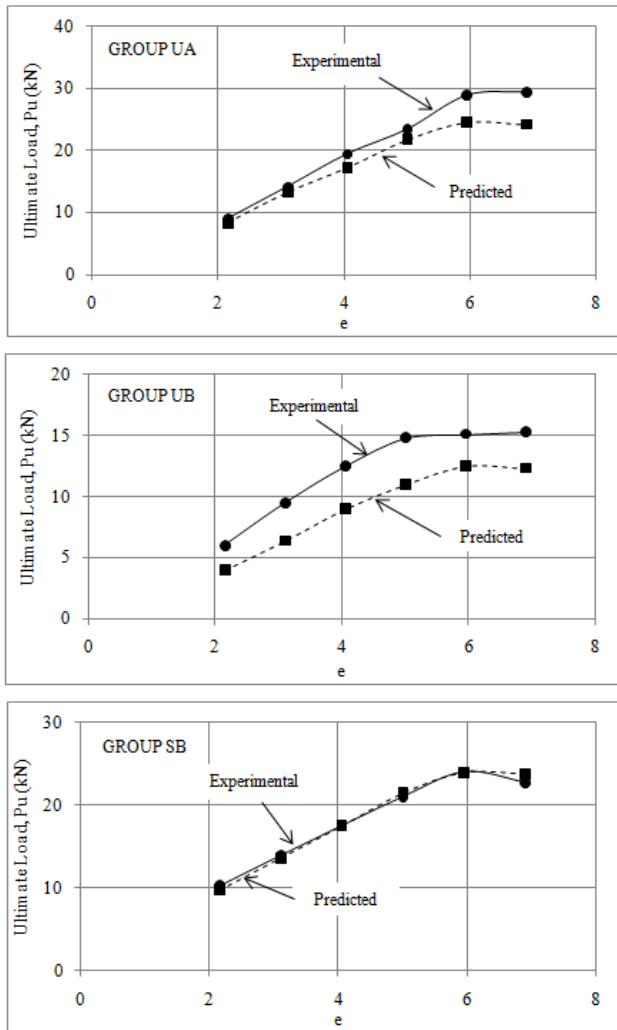


Fig. 8 Comparison between experimental and calculated trends of joint strengths

UB as compared to those in Group UA or SB. The ratio of experimental to calculated ultimate strength for these specimens ranges from 1.59 to 1.23 (Table 3).

The main reasons for the highly conservative predictions of strength for specimens in Group UB may be attributed to the strain hardening of reinforcement. Since the volume fraction of reinforcement was low, the specimen demonstrated considerable deformability as shown in Fig. 6 allowing the steel strain to reach the hardening zone. Indeed, the ratio of ultimate strength to yield strength of 1.24 (Table 2) for mesh reinforcement supports this observation.

The results of all 28 tests reported herein are compared with the respective theoretical predictions in Table 3. It may be seen that the theoretical predictions are, in general, conservative. The ratio of experimental to calculated ultimate strengths ranges from 0.95 to 1.59 with an average of 1.17 and standard deviation of 0.16. As mentioned earlier, the specimens containing low volume fraction of reinforcement demonstrated high values of the ratio of experimental to calculated joint strength due to strain hardening of reinforcement associated with large deformation.

5. Conclusions

Within the scope of investigation, the following are the conclusions drawn in this study:

- (1) With the increase in the edge distance the strength of the bolted shear joints was found to increase with the consequent changes in the mode of failure. This increase was, however, terminated by the upper bound on the joint strength as dictated by either tension or bearing failure.
- (2) For a given edge distance, an increase in the volume fraction of reinforcement has been shown to be associated with an increase in the capacity of the joint.
- (3) It has been possible to enhance the joint capacity by using simple U-inserts around the bolt hole. The strength can be enhanced further by increasing the diameter of insert wire.
- (4) The joint capacity was found to increase as the distance between the outstanding legs of U-inserts was increased up to half the width of ferrocement plate. However, the effect of the location of insert from the edge of the plate remains inconclusive.
- (5) The effect of U-insert may be analytically integrated in the strength calculation which has been found to give good and safe predictions of strength for the joints in assembling precast ferrocement structures.

References

- Abdul Awal, A.S. (1988), "Failure mechanism of prepacked concrete", *J. Struct. Eng.*, **114**(3), 727-732.
- Abdullah, M.M. and Alwis, W. (1994), "Strength of bolted joints in ferrocement", *Struct. J.*, **91**(3), 315-323.
- Andalib, Z., Kafi, M.A. and Bazzaz, M. (2010), "Using hyper elastic material for increasing ductility of bracing", *Proceedings of the 1st Conference of Steel & Structures and 2nd Conference on Application of High-Strength Steels in Structural Industry, Steel & Structures*.
- Andalib, Z., Kafi, M.A., Kheyroddin, A. and Bazzaz, M. (2011), "Investigation on the Ductility and Absorption of Energy of Steel Ring in Concentric Braces", *Proceedings of the 2nd Conference of Steel and Structures, Steel and Structures*.
- Balaguru, P. and Batson, G. (1997), "State-of-the-art Report on Ferrocement", ACI Committee, **549**.
- Bazzaz, M. (2010), *Seismic Behavior of Off-Centre Braced Frame with Circular Element in Steel Frame Design*, Semnan University.
- Bazzaz, M., Kafi, M.A., Andalib, Z. and Esmaili, H. (2011a), "Seismic Behavior of Off-centre Bracing Frame", *Proceedings of the 6th National Congress on Civil Engineering*.
- Bazzaz, M., Kheyroddin, A., Kafi, M.A. and Andalib, Z. (2011b), "Evaluating the performance of steel ring in special bracing frame", *Proceedings of the 6th Seismology and Earthquake Engineering International Conference*, Ministry of Science, Research and Technology, Tehran Iran.
- Bazzaz, M., Kheyroddin, A., Kafi, M.A. and Andalib, Z. (2012a), "Evaluation of the seismic performance of off-centre bracing system with ductile element in steel frames", *Steel Compos. Struct., Int. J.*, **12**(5), 445-464.
- Bazzaz, M., Kheyroddin, A., Kafi, M.A. and Andalib, Z. (2012b), "Modeling and Analysis of Steel Ring Devised in Off-centric

- Braced Frame with the Goal of Improving Ductility of Bracing Systems”, Iran Scientific and Industrial Researches Organization, Tehran, Iran.
- Bazzaz, M., Kafi, M.A., Kheyroddin, A., Andalib, Z. and Esmaeili, H. (2014), “Evaluating the seismic performance of off-centre bracing system with circular element in optimum place”, *Int. J. Steel Struct.*, **14**(2), 293-304.
- Bazzaz, M., Andalib, Z., Kheyroddin, A. and Kafi, M.A. (2015), “Numerical comparison of the seismic performance of steel rings in off-centre bracing system and diagonal bracing system”, *Steel Compos. Struct., Int. J.*, **19**(4), 917-937.
- Fanaie, N., Aghajani, S. and Shamloo, S. (2012), “Theoretical assessment of wire rope bracing system with soft central cylinder”, *Proceedings of the 15th World Conference on Earthquake Engineering*.
- Fanaie, N., Esfahani, F.G. and Soroushnia, S. (2015), “Analytical study of composite beams with different arrangements of channel shear connectors”, *Steel Compos. Struct., Int. J.*, **19**(2), 485-501.
- Fanaie, N., Aghajani, S. and Afsar Dizaj, E. (2016a), “Strengthening of moment-resisting frame using cable-cylinder bracing”, *Adv. Struct. Eng.*, **19**(11), 1736-1754.
- Fanaie, N., Aghajani, S. and Dizaj, E.A. (2016b), “Theoretical assessment of the behavior of cable bracing system with central steel cylinder”, *Adv. Struct. Eng.*, **19**(3), 463-472.
- Guo, X., Huang, Z., Xiong, Z., Yang, S. and Peng, L. (2016a), “Experimental studies on behaviour of bolted ball-cylinder joints under axial force”, *Steel Compos. Struct., Int. J.*, **21**(1), 137-156.
- Guo, X.N., Huang, Z.W., Xiong, Z., Yang, S. and Peng, L. (2016b), “Numerical studies on behaviour of bolted ball-cylinder joint under axial force”, *Steel Compos. Struct., Int. J.*, **20**(6), 1323-1343.
- Hammoud, H. and Naaman, A. (1998), “Ferrocement bolted shear joints: Failure modes and strength prediction”, *Cement Concrete Compos.*, **20**(1), 13-29.
- Hammoud, H. and Naaman, A. (2000), “Ferrocement bolted shear joints: Finite element analysis and stress distribution”, *J. Ferrocement*, **30**(1), 31-43.
- Heydari, A. and Shariati, M. (2018), “Buckling analysis of tapered BDFGM nano-beam under variable axial compression resting on elastic medium”, *Struct. Eng. Mech., Int. J.*, **66**(6), 737-748.
- Hosseinpour, E., Baharom, S., Badaruzzaman, W.H.W., Shariati, M. and Jalali, A. (2018), “Direct shear behavior of concrete filled hollow steel tube shear connector for slim-floor steel beams”, *Steel Compos. Struct., Int. J.*, **26**(4), 485-499.
- Jamkhaneh, M.E. and Kafi, M.A. (2017), “Experimental and numerical investigation of octagonal partially encased composite columns subject to axial and torsion moment loading”, *Civil Eng. J.*, **3**(10), 939-955.
- Katula, L. and Dunai, L. (2015), “Experimental study on standard and innovative bolted end-plate beam-to-beam joints under bending”, *Steel Compos. Struct., Int. J.*, **18**(6), 1423-1450.
- Khorami, M., Alvansazyazdi, M., Shariati, M., Zandi, Y., Jalali, A. and Tahir, M. (2017a), “Seismic performance evaluation of buckling restrained braced frames (BRBF) using incremental nonlinear dynamic analysis method (IDA)”, *Earthq. Struct., Int. J.*, **13**(6), 531-538.
- Khorami, M., Khorami, M., Motahar, H., Alvansazyazdi, M., Shariati, M., Jalali, A. and Tahir, M.M. (2017b), “Evaluation of the seismic performance of special moment frames using incremental nonlinear dynamic analysis”, *Struct. Eng. Mech., Int. J.*, **63**(2), 259-268.
- Khorramian, K., Maleki, S., Shariati, M. and Sulong, N.R. (2015), “Behavior of Tilted Angle Shear Connectors”, *PLoS one*, **10**(12), 1-11.
- Khorramian, K., Maleki, S., Shariati, M., Jalali, A. and Tahir, M.M. (2017), “Numerical analysis of tilted angle shear connectors in steel-concrete composite systems”, *Steel Compos. Struct., Int. J.*, **23**(1), 67-85.
- Krishnamoorthy, T.S., Parameswaran, V.S., Neelamegam, M. and Balasubramanian, K. (1990), “Investigation of precast ferrocement planks connected by steel bolts”, *Special Publication*, **124**, 389-404.
- Ksentini, O., Combes, B., Abbes, M.S., Daidie, A. and Haddar, M. (2015), “Simplified model to study the dynamic behaviour of a bolted joint and its self loosening”, *Struct. Eng. Mech., Int. J.*, **55**(3), 639-654.
- Li, B., Lam, E.S.S., Wu, B. and Wang, Y.Y. (2013), “Experimental investigation on reinforced concrete interior beam-column joints rehabilitated by ferrocement jackets”, *Eng. Struct.*, **56**, 897-909.
- Li, S., Li, Q., Jiang, H., Zhang, H., Yan, L. and Jiang, W. (2018), “Experimental study on a new type of assembly bolted end-plate connection”, *Steel Compos. Struct., Int. J.*, **26**(4), 463-471.
- Lopez-Arancibia, A., Altuna-Zugasti, A.M., Aldasoro, H.A. and Pradera-Mallabiarrena, A. (2015), “Bolted joints for single-layer structures: numerical analysis of the bending behaviour”, *Struct. Eng. Mech., Int. J.*, **56**(3), 355-367.
- Ma, H., Li, S., Li, Z., Liu, Y., Dong, J. and Zhang, P. (2018), “Shear behavior of composite frame inner joints of SRRC column-steel beam subjected to cyclic loading”, *Steel Compos. Struct., Int. J.*, **27**(4), 495-508.
- Mansouri, I., Safa, M., Ibrahim, Z., Kisi, O., Tahir, M.M., Baharom, S. and Azimi, M. (2016), “Strength prediction of rotary brace damper using MLR and MARS”, *Struct. Eng. Mech., Int. J.*, **60**(3), 471-488.
- Mansur, M. (1995), “An investigation into the behavior and strength of bolted connections in ferrocement”, *J. Ferrocement*, **25**(3), 207-219.
- Mansur, M.A., Paramasivam, P. and Lee, S.L. (1987), “Ferrocement Sunscreens on High-Rise Buildings”, *Concrete Int.*, **9**(9), 19-23.
- Mansur, M.A., Tan, K.L., Naaman, A.E. and Paramasivam, P. (2001), “Bolt bearing strength of thin-walled ferrocement”, *Struct. J.*, **98**(4), 563-571.
- Mohammadhassani, M., Nezamabadi-Pour, H., Suhatri, M. and Shariati, M. (2013), “Identification of a suitable ANN architecture in predicting strain in tie section of concrete deep beams”, *Struct. Eng. Mech., Int. J.*, **46**(6), 853-868.
- Mohammadhassani, M., Nezamabadi-Pour, H., Suhatri, M. and Shariati, M. (2014), “An evolutionary fuzzy modelling approach and comparison of different methods for shear strength prediction of high-strength concrete beams without stirrups”, *Smart Struct. Syst., Int. J.*, **14**(5), 785-809.
- Mohammadhassani, M., Saleh, A., Suhatri, M. and Safa, M. (2015), “Fuzzy modelling approach for shear strength prediction of RC deep beams”, *Smart Struct. Syst., Int. J.*, **16**(3), 497-519.
- Momenzadeh, S., Seker, O., Faytarouni, M. and Shen, J. (2017), “Seismic performance of all-steel buckling-controlled braces with various cross-sections”, *J. Constr. Steel Res.*, **139**, 44-61.
- Mourad, S.M. and Shannag, M.J. (2012), “Repair and strengthening of reinforced concrete square columns using ferrocement jackets”, *Cement Concrete Compos.*, **34**(2), 288-294.
- Murali, D. (1997), “Use of precast concrete wall and slab with bolted joints for buildings”, *Indian Concrete J.*, **71**, 73-78.
- Naaman, A.E. (1989), “Ferrocement housing: toward integrated high technology solutions”, *J. Ferrocement*, **19**(2), 141-149.
- Naaman, A.E. (2000), *Ferrocement and Laminated Cementitious Composites*, Techno press MI.
- Naaman, A.E. and Hammoud, H. (1992), “Ferrocement prefabricated housing: the next generation”, *J. Ferrocement*, **22**(1), 35-47.

- Safa, M., Shariati, M., Ibrahim, Z., Toghroli, A., Baharom, S.B., Nor, N.M. and Petkovic, D. (2016), "Potential of adaptive neuro fuzzy inference system for evaluating the factors affecting steel-concrete composite beam's shear strength", *Steel Compos. Struct., Int. J.*, **21**(3), 679-688.
- Shah, A.A. (2011), "Applications of ferrocement in strengthening of unreinforced masonry columns", *Int. J. Geol.*, **5**(1), 21-27.
- Shahabi, S.E.M., Sulong, N.H., Shariati, M., Mohammadhassani, M. and Shah, S.N.R. (2016), "Numerical analysis of channel connectors under fire and a comparison of performance with different types of shear connectors subjected to fire", *Steel Compos. Struct., Int. J.*, **20**(3), 651-669.
- Shariati, M. (2013), "Behaviour of C-shaped shear connectors in steel concrete composite beams", Ph.D. Thesis; Faculty of engineering University of Malaya, Kuala Lumpur, Malaysia.
- Shariati, M., Sulong, N.R., Suhatri, M., Shariati, A., Khanouki, M.A. and Sinaei, H. (2013), "Comparison of behaviour between channel and angle shear connectors under monotonic and fully reversed cyclic loading", *Constr. Buil. Mater.*, **38**, 582-593.
- Shariati, A., Shariati, M., Sulong, N.R., Suhatri, M., Khanouki, M.A. and Mahoutian, M. (2014a), "Experimental assessment of angle shear connectors under monotonic and fully reversed cyclic loading in high strength concrete", *Constr. Build. Mater.*, **52**, 276-283.
- Shariati, M., Shariati, A., Sulong, N.R., Suhatri, M. and Khanouki, M.A. (2014b), "Fatigue energy dissipation and failure analysis of angle shear connectors embedded in high strength concrete", *Eng. Fail. Anal.*, **41**, 124-134.
- Shariati, M., Sulong, N.R., Shariati, A. and Khanouki, M.A. (2015), "Behavior of V-shaped angle shear connectors: experimental and parametric study", *Mater. Struct.*, **49**(9), 3909-3926.
- Shariati, M., Sulong, N.R., Shariati, A. and Kueh, A.B.H. (2016), "Comparative performance of channel and angle shear connectors in high strength concrete composites: An experimental study", *Constr. Buil. Mater.*, **120**, 382-392.
- Shariati, M., Tahir, M.M., Wee, T.C., Shah, S.N.R., Jalali, A., Abdullahi, M.A.M. and Khorami, M. (2018), "Experimental investigations on monotonic and cyclic behavior of steel pallet rack connections", *Eng. Fail. Anal.*, **85**, 149-166.
- Stanojevic, D., Mandic, M., Danon, G. and Svrzic, S. (2017), "Prediction of the surface roughness of wood for machining", *J. Forestry Res.*, **28**(6), 1281-1283.
- Tahmasbi, F., Maleki, S., Shariati, M., Sulong, N.R. and Tahir, M.M. (2016), "Shear capacity of C-shaped and L-shaped angle shear connectors", *PloS one*, **11**(8), e0156989.
- Toghroli, A., Mohammadhassani, M., Suhatri, M., Shariati, M. and Ibrahim, Z. (2014), "Prediction of shear capacity of channel shear connectors using the ANFIS model", *Steel Compos. Struct., Int. J.*, **17**(5), 623-639.
- Toghroli, A., Suhatri, M., Ibrahim, Z., Safa, M., Shariati, M. and Shamshirband, S. (2016), "Potential of soft computing approach for evaluating the factors affecting the capacity of steel-concrete composite beam", *J. Intel. Manuf.*, 1-9.
- Toghroli, A., Darvishmoghaddam, E., Zandi, Y., Parvan, M., Safa, M., Abdullahi, M.A.M., Heydari, A., Wakil, K., Gebreel, S.A. and Khorami, M. (2018), "Evaluation of the parameters affecting the Schmidt rebound hammer reading using ANFIS method", *Comput. Concrete, Int. J.*, **21**(5), 525-530.